

Solar cell split source inverter for induction motor with computer control

Omer N. Mahmood¹, Salam R. Mehdi², Khalaf S. Gaeid¹, Atheer L. Salih Al-Tameemi³

¹Department of Electrical Engineering, Tikrit University, Tikrit, Iraq

²RAM General Express LLC, and Home Health Care LLC in Ohio, Ohio, USA

³Department of Electrical Engineering Department, School of Engineering, Baden-Wuerttemberg Cooperative State University, Ravensburg, Germany

Article Info

Article history:

Received Apr 8, 2022

Revised Nov 24, 2022

Accepted Dec 6, 2022

Keywords:

Computer modeling

Induction motor

LC filter

Maximum power point tracking

Photovoltaic PV

Split source inverter

ABSTRACT

The electrical energy is necessary for daily life, but there is a continuous increase in the usage rate of electric energy. Such an increase is a big problem, which makes us think about using alternative energy for conventional energy, in addition to the problem of pollution resulting from the use of energy generation. Solar energy is a solution for energy in terms of consumption, besides there is no environmental risk in the use of solar energy. In this work, an integrated solar system operating in the daytime has been designed to operate a 3-phase induction motor (IM). The study begins by simulating the system in the MATLAB/Simulink program in order to find out the results and verify them using the same components of the proposed algorithm. The system with photovoltaic (PV) modules 1080 W, whereas the PV array is a direct source of the designed split source inverter (SSI). This SSI is controlled by sine pulse width modulation (SPWM). The maximum power point tracking (MPPT) incremental conductance (INC) method is monitored by a computer connected to the system via a Wi-Fi connection, the 3-phase IM (373) W. The results reveal the efficiency of the system and that it can be versatile.

This is an open access article under the [CC BY-SA](https://creativecommons.org/licenses/by-sa/4.0/) license.



Corresponding Author:

Khalaf S. Gaeid

Department of Electrical Engineering, Tikrit University, Tikrit, Iraq

Email: gaeidkhalaf@gmail.com

1. INTRODUCTION

One of the wonderful solutions to the increasing depletion of fossil fuels is the alternative energy, which is renewable energy [1], [2]. Including solar energy, to meet the demands of energy used in daily industries, agriculture and irrigation, as well as the population's energy use. And all this is due to reliability and lack of maintenance [3], [4]. Controlling the speed of the induction motor (IM) is one of the most important requirements for the IM [5]. The frequency is variable as the speed is dependent on speed of the rotor field made available by the stator. Likewise, Additionally, a variable voltage is needed [6]. This method is called V/f method. The inverter is equipped with panels and the inverter in turn feeds the IM. In Figure 1 the proposed system for controlling the speed of rotation of the IM is illustrated.

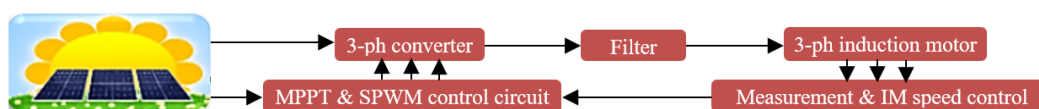


Figure 1. The proposed solar system diagram

2. MATERIALS AND METHODS

2.1. Solar energy

PV energy is a significant electric energy solution. As a study case, by understanding the amounts of solar radiation that fall on various places throughout the year, it is feasible to evaluate Iraq's potential for PV energy, when the monthly averages of a solar radiation total that falls on the horizontal surface of every location in Iraq are discovered [7], [8]. Figure 2 depicts that these rates are at their highest irradiance (W/m^2) during winter. These rates are at their maximum during the summer. Figure 3 displays the annual spatial distribution of solar irradiance from Iraq. In general, these numbers show that Iraq is rich in solar energy in all locations, which may be invested in a variety of solar energy applications [9]. The photoelectric system has several advantages, including high dependability because it is a free source and low maintenance because its pieces are permanent.

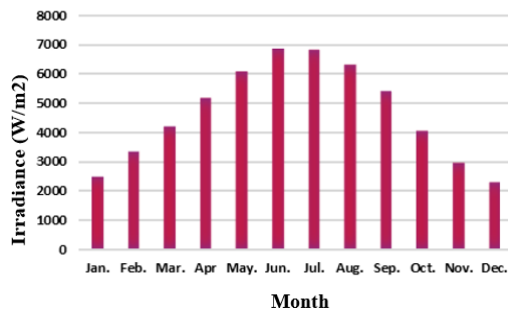


Figure 2. Average solar irradiance(horizontal) vs months

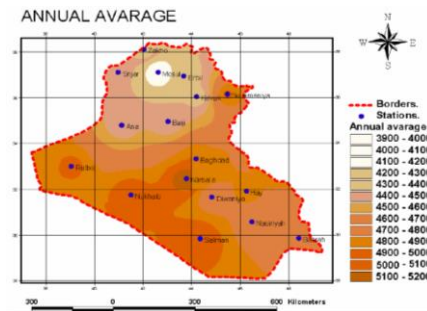


Figure 3. Yearly sun radiation in Iraq

2.2. Algorithms for MPPT

To boost the solar system's energy effectiveness, the maximum power point tracking (MPPT) formula is utilized. MPPT can really be accomplished in a variety of ways. The INC approach was used in this research. MPPT is implemented through INC method it's shown in Figure 4. Figure 5 displays the current and power as the MPPT algorithm is applied to various radiation values.

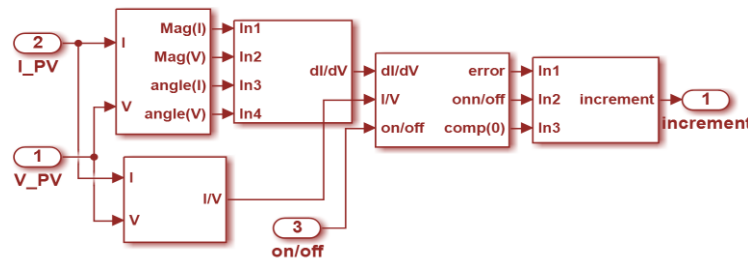


Figure 4. Method scheme of INC method

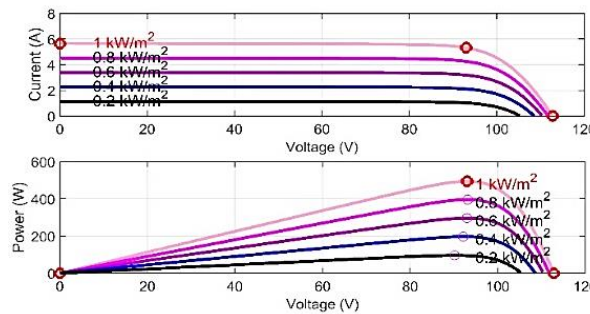


Figure 5. MPPT algorithm to various irradiation values

The INC approach is predicated on the notion that PV output's power derivative is equal to 0. The outputs of this technique are virtually effective in quick switching situations when the PV radiation is reduced, the MPP moves to the left. This approach is regarded as one of best in regards to performance, but it is expensive and has a complicated control circuit. An MPPT system's optimal performance specifications include sufficient tracking precision, speed, minimal steady-state error, and high efficiency [10]. The ratio of generated solar energy to voltage obtained in MPPT via INC method is zero, as shown in (1).

$$dP/dV = 0 \quad (1)$$

$$P = V * I \quad (2)$$

$$\frac{d(V*I)}{dV} = I + V * dI/dV = 0 \quad (3)$$

$$\frac{dI}{dV} = -I/V$$

$$dI/dV = -I /V \quad (4)$$

Where dV , dI is harmonic of voltage (V) and current (I). I , V is voltage (V) and current (I). Error is expressed as (5):

$$\frac{dI}{dV} + I/V \approx 0 \quad (5)$$

2.3. PV computer modeling

When the photon energy hits a PV cell's surface, it absorbs it and releases energy-carrying electrons, which spin through an external load in a closed loop circuit to provide the cell with energy [11], [12]. An essential PV performance is shunt resistance (RSH). The leakage current across the load circuit is plainly reduced. According to various electrical parameters, the nearby cells' leakage currents define the matrix's output power, while a single cell's local heating causes a cell to degrade. Al Juheshi [13] talks about the impact of parallel leakage current resistance. Figure 6 shows A PV cell's modeling.

$$I = I_L - I_d - I_{sh} \quad (6)$$

Where I , I_L , I_d , I_{sh} is the output current, photocurrent, diode current, the current leak in the parallel resistance respectively. These mathematical equations describe how the light generated current fluctuates with temperature and irradiance:

$$I = I_L - I_s \left[\exp\left(\frac{(V+I.R_s)q}{akT N_s} - 1\right) - \frac{(V+I.R_s)}{R_{sh}} \right] \quad (7)$$

$$I_L = I_r \frac{I_{sc}}{I_{r0}} \quad (8)$$

$$I_s = I_{sc} / \left[\exp\left(\frac{V_{oc}}{aV_t} - 1\right) \right] \quad (9)$$

$$I_d = I_s / \left[\exp\left(\frac{V+I.R_s}{aV_t} - 1\right) \right] \quad (10)$$

$$I_{sh} = (V + I.R_s) / R_{sh} \quad (11)$$

$$V_t = kT N_s / q \quad (12)$$

where N_s , I_L , I_s , R_s and R_{sh} represent the number of series connected cells, light generated current, the reverse saturation current, the series resistances and parallel resistance of cell respectively. The electron charge $q=1.60217646 \times 10^{-19}$ C, Boltzmann's constant $k=1.3806503 \times 10^{-23}$ J/K, ideality factor modified is a.

$$P_m = I_m V_m = FF * I_{sc} V_{sc} \quad (13)$$

Where FF , Im , and Vm are, respectively, the fill factor, a reliability indicator, a maximum current, and a maximum voltage.

$$FF = P_{max}/P_{theoretical} \tag{14}$$

Where P_{in} , P_{out} the input power and output power.

$$P_{out} = P_{max} (W/m^2) \tag{15}$$

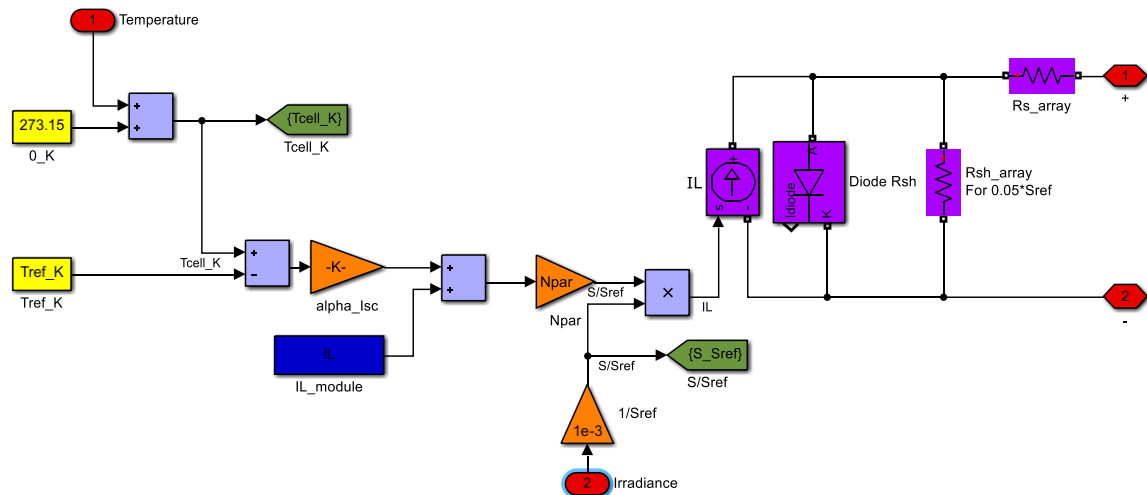


Figure 6. A PV cell's modeling

2.4. Speed computer control IM

In multiple industries over the years, including paper mills, factories, steel and cement plants, robots, and wind power systems, IM has been widely used. because of its easy maintenance, great longevity, and straightforward and stable structure. The control system is depicted in Figure 6 as consisting of an IM controller, an inverter, a sensor, and an IM [14]. The rotor speed control method in IM via the V/f control method is shown in Figure 7. Based on the reference frequency (f_s^*), standard control IM determines the stator voltage as follows:

$$V_s^* = \left(\frac{V_n - V_{min}}{f_n - f_{min}} \right) f_s^* \tag{16}$$

V_{min} , V_n , f_{min} and f_n are the minimum voltage, rated voltage, minimum frequency, rated frequency. The reference voltage formulas are:

$$V_\alpha^* = V_s^* \cos(2\pi f_s^* t) \tag{17}$$

$$V_\beta^* = V_s^* \sin(2\pi f_s^* t) \tag{18}$$

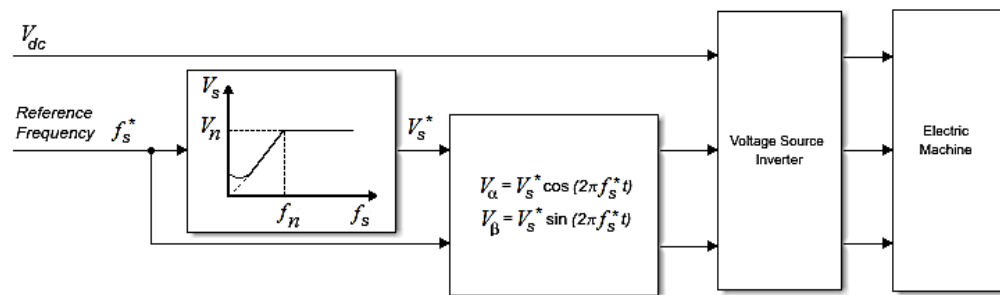


Figure 7. Scheme of V/f Control method

In this study, an inverter with a PWM sinusoidal voltage supply and an induction motor were controlled by a computer using a mathematical model of the system. It is suggested to use a single-phase PV system with a three-phase IM motor. The PWM to MPPT control method from sunlight is combined with the stroke control algorithm in the discrete system. Figure 8 depicts the PWM implementation used in this investigation using MATLAB/Simulink.

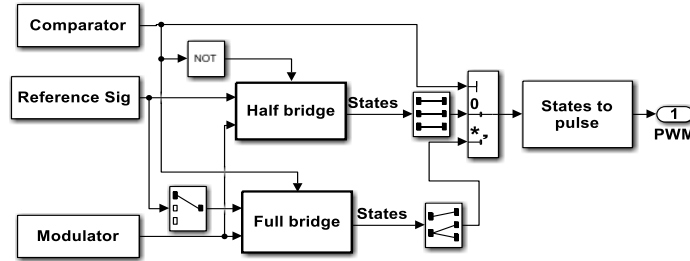


Figure 8. SPWM generation technique

The mathematical model of the IM in the direct quadrature dq-reference frame.

$$\begin{bmatrix} i_{sd} \\ i_{sq} \\ i_{rd} \\ i_{rq} \end{bmatrix} = \frac{1}{L_m^2 - L_s L_r} \left(A \begin{bmatrix} i_{sd} \\ i_{sq} \\ i_{rd} \\ i_{rq} \end{bmatrix} + \begin{bmatrix} L_s & 0 & L_m & 0 \\ 0 & L_r & 0 & L_m \\ L_m & 0 & L_r & 0 \\ 0 & L_m & 0 & L_r \end{bmatrix} * \begin{bmatrix} v_{sd} \\ v_{sq} \\ v_{rd} \\ v_{rq} \end{bmatrix} \right) A = \begin{bmatrix} \frac{-(R_s + R_r (L_m / \tau_r)^2)}{\sigma L_s} & 0 & \frac{L_m}{\sigma L_s L_r \tau_r} & \frac{\omega_r L_m}{\sigma L_s L_r} \\ 0 & \frac{-(R_s + R_r (L_m / \tau_r)^2)}{\sigma L_s} & \frac{-\omega_r L_m}{\sigma L_s L_r} & \frac{L_m}{\sigma L_s L_r \tau_r} \\ L_m / \tau_r & 0 & -1 / \tau_r & -\omega_r \\ 0 & L_m / \tau_r & \omega_r & -1 / \tau_r \end{bmatrix}$$

Where ω_r , τ_r , L_s , L_r , L_m , σ and are IM velocity (rad/s), rotor time, stator inductance, rotor inductance, mutual inductance, leakage coefficient [15].

The structure of the inverter consists of passive components, diodes and insulated-gate-bipolar transistors (IGBTs). Figure 9 shows SSI in MATLAB/Simulink. The SSI is using the same bridge as a voltage-source inverter (VSI). Two components make up the SSI impedance network: a capacitor (C) linked in parallel to the inverter bridge and an inductor (L) connected in series to the DC source [16]. Three diodes link the three inductors to each bridge leg's switch node. The SSI charges L in impedance network to use the lowest switches of a bridge, The higher switches diodes are then utilized to discharge L and charge C where at minimum one switch is engaged for charging. while every lower switch is off. scalar control, INC MPPT, and SPWM generator are all included in inverting control. Inverter control is seen in Figure 10. MPPT increment is 0.01 V, upper and lower outputs limits are (104,75) V, and the output beginning value (V) is (105) V. In Figure 11, the gate pulse from SPWM is seen.

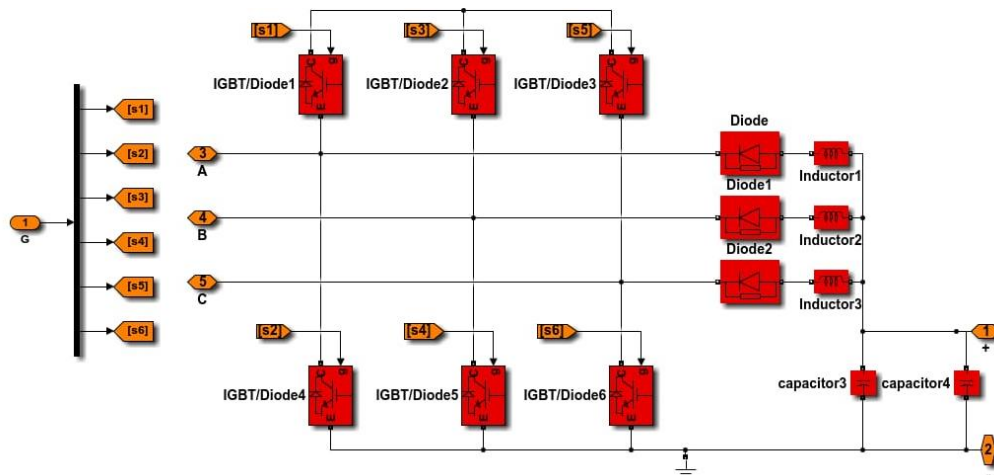


Figure 9. The structure of the SSI

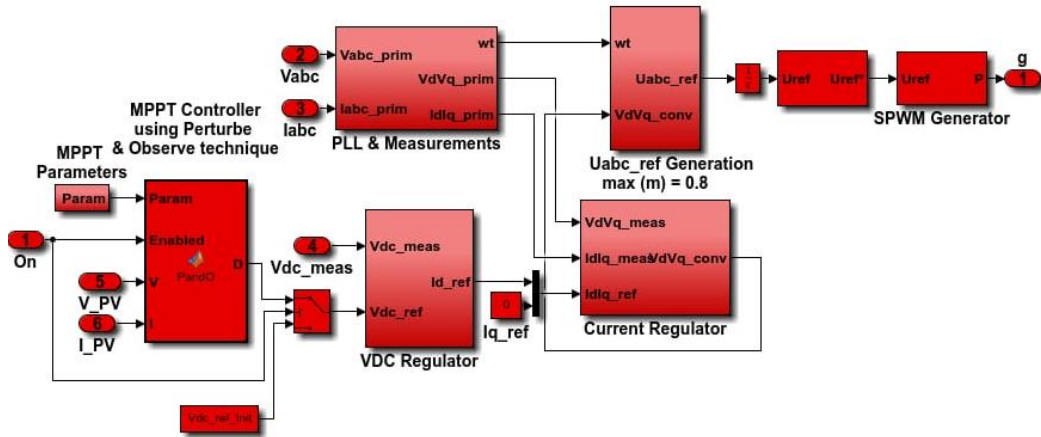


Figure 10. Inverter control

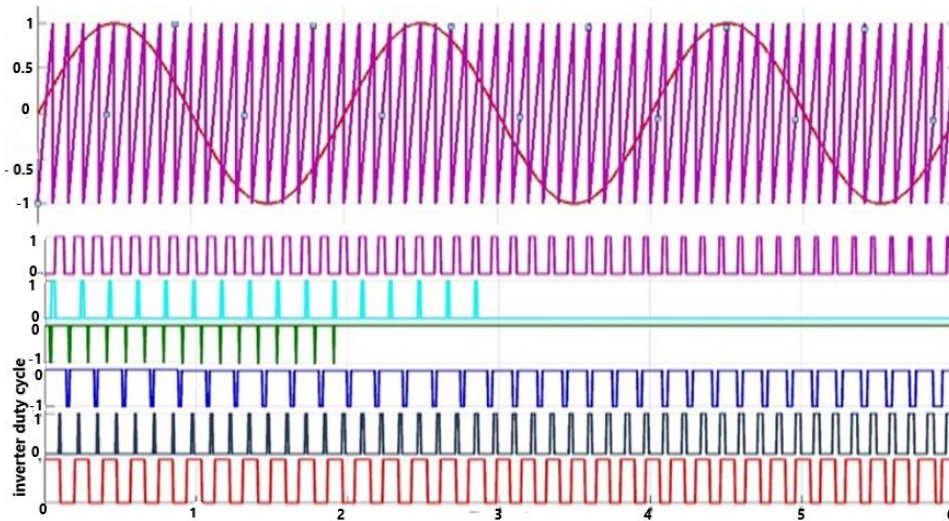


Figure 11. Gates pulse

Switches on any leg (S_5 and S_2 , S_1 and S_4 , S_3 and S_6 , where $S_1 + S_6 = 1$, $S_3 + S_4 = 1$ and $S_5 + S_2 = 1$) cannot be switched on together in single-phase VSI [17].

$$Vdc/2(S_1 - S_6) = V_{an} + V_{no} \tag{19}$$

$$Vdc/2(S_3 - S_4) = V_{bn} + V_{no} \tag{20}$$

$$Vdc/2(S_5 - S_2) = V_{cn} + V_{no} \tag{21}$$

The load's phase voltages are V_{an} , V_{cn} and V_{bn} and its neutral voltage relative to inverter base is V_{no} .

$$Vdc/2(M_1) = V_{an} + V_{no} \tag{22}$$

$$Vdc/2(M_3) = V_{bn} + V_{no} \tag{23}$$

$$Vdc/2(M_5) = V_{cn} + V_{no} \tag{24}$$

Where M is the modulation signal.

$$M = m \sin(\omega t + \varphi) \tag{25}$$

Where φ signal phase just at the beginning of the reference period is and (m) modulation index may vary from 1 to 0. The (26) is created by adding (19) through (21) as follows:

$$V_{dc}/2[(S_5 + S_3 + S_1) - (S_6 + S_4 + S_2)] = V_{an} + V_{bn} + V_{cn} + 3V_{no} \quad (26)$$

$$V_{no} = V_{dc}/2[2S_1 + 2S_3 + 2S_5 - 3] \quad (27)$$

altering the operating frequency in order to manage synchronous speed. The stator contains the induced voltage is $E1 \propto \Phi f$, Φ is the flux air gap and f is frequency. You may disregard the stators voltage drop and obtain the line voltage $V \propto \Phi f$. To keep a consistent V/f ratio, the voltage varies whenever the frequency is adjusted to regulate the IM speed. For different f values within the operating range, the maximum torque remains as is the case with different speed [18].

2.5. LC filter

One of filtering chamber that combines the options (C and L) is this one. It is effective and has a large enough ripple reduction factor. A perfect process filter may be created by combining the capacitor's job of stabilizing voltage with inductor filter's work of smoothing the current [19]. Figure 12 depicts an LC filter and its output voltage. The Thevenin circuit for LC filter connected between IM and SSI are shown in Figure 13.

$$L_{eq} = \frac{[L_f*(L_s+L_r)]}{[L_f+(L_s+L_r)]} \quad (28)$$

It was decided to use an L filter so that drop voltage would be less than 3%. C that is selected so that FC falls below the conversion frequency of one-third [20], [21].

$$L_{eq} = \frac{0.03*v_{inv}}{2\pi f I_{Lmax}} \quad (29)$$

I_{Lmax} : Peak current of inductor.



Figure 12. LC filter

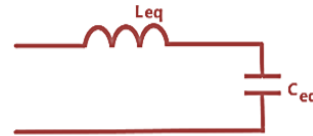


Figure 13. Equivalent of Thevenin LC filter

3. RESULTS

In order to evaluate the performance of the proposed system, computer simulations using MATLAB/Simulink have been performed using IM of (373) W, whose parameters are listed in Table 1. The system has also been implemented in practical. Table 2 shows a closed loop V/f IM control result.

The MATLAB/Simulink implementation of proposed algorithm is seen in Figure 14 while Figure 15 shows the hardware setup of the proposed system. The PV entry temperature may be adjusted from 0 to (25) °C. Additionally, the amount of solar radiation that enters the PV may be adjusted from zero to (1000) W/m². The collection of PV panels transforms solar energy into DC current as in [22]. In order to design PCB boards, they were initially simulated in proteus v8.9 [23]. The final simulation was obtained in a 3D visualizer. The component used in control board is STM32F334R8T6 Microcontrollers [24], [25].

Table 1. IM parameters

Values	Quantity
373W	Power
50 Hz	Supply frequency
1440 RPM	Rated speed
2	No. of pair poles
15 Ω	Rotor resistance
20 Ω	Stator resistance
0.98 H	Rotor inductance
0.98 H	Stator inductance
0.922 H	Mutual inductance

Table 2. Results of closed loop V/f control

VDC	VAC	f	V/f
104	69.2	15	4.61
104	92.0	20	4.60
104	116.0	25	4.64
104	137.5	30	4.58
104	162.1	35	4.63
104	184.3	40	4.60
104	207.9	45	4.62
104	230	50	4.60

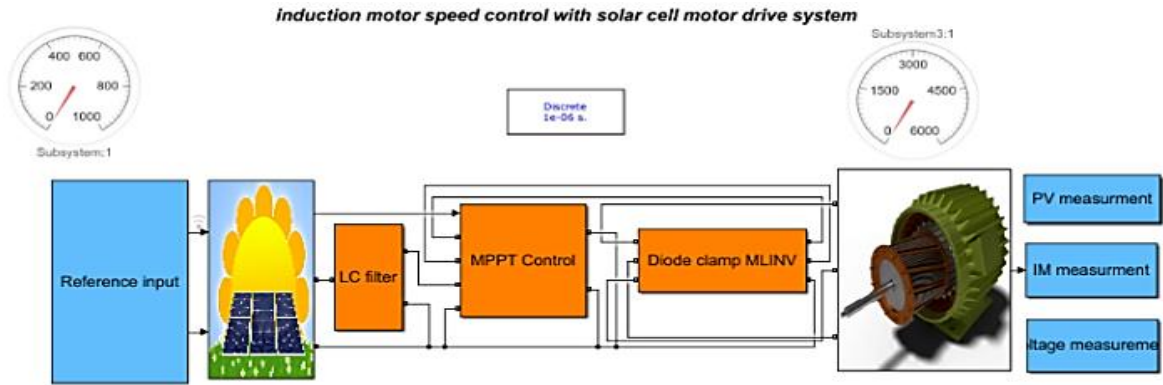


Figure 14. Simulink implementation of the proposed algorithm



Figure 15. Hardware setup of the PV system

Figure 16 illustrates a simplified block diagram of the controlled system. The plant including the power circuit, PV, and current transducer is modeled as a second-order transfer function given. The system response of the considered closed loop system is shown in Table 3.

A pure sine signal must be obtained by adding filter after inverter circuit, as shown in Figure 17, because voltage before the filter is not a sine wave. The outcome of feeding the inverter's output into the filter is a clean sinusoidal voltage ranging from (250 V to -250 V). The output filter is simulated, and the results are shown in Figure 18.

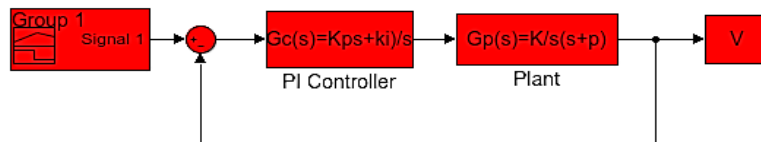


Figure 16. Block diagram of feedback control system

Table 3. System response

Gain k	Max. overshoot	Rise-time (sec)	Steady state error
10	3	1.1	0.08

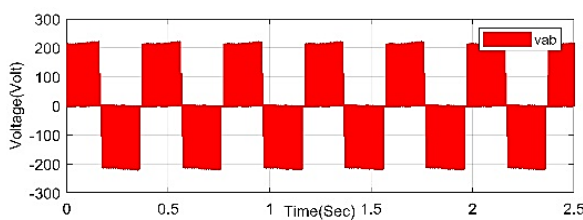


Figure 17. Inverter voltage with three levels

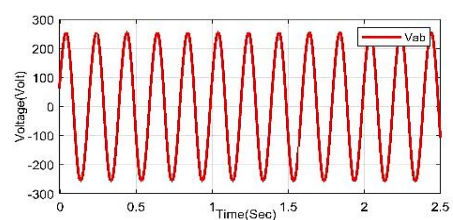


Figure 18. Output waveform after the LC filter

The IM's torque is fixed at 4 Nm lasting less than one second after the brief response, as seen in Figure 19. To guarantee an increase in IM efficiency in steady-state zone that starts roughly after the first second, the suggested system torque substantially drops by 50% during (0.25s to 0.75s). The IM reference speed is (1440) RPM is shown in Figure 20. The IM's rotor current is fixed on 2Amp after transient response fewer than 1s as seen in Figure 21, same for the stator current seen in Figure 22. At startup, the IM stator current is around (10) Amp, then it steadily drops until it achieves a current of (2.5) Amp.

Peak-to-peak voltage phase at a frequency of (50) Hz is shown in Figure 23, with a voltage level of (576)V. Line current are displayed in Figure 24. The current value (2.75) Amp. PV voltage is seen in Figure 25 at 1:00 p.m. The voltage at this moment have a value of(104) V. The oscilloscope-measured portion of the S2 and S5 SPWM is shown in Figure 26.

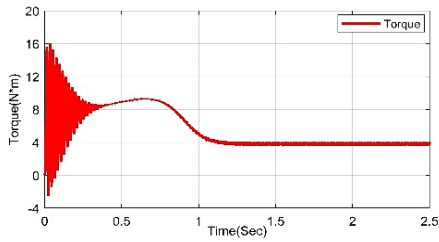


Figure 19. Torque of the IM

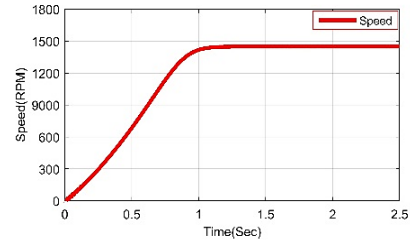


Figure 20. IM speed

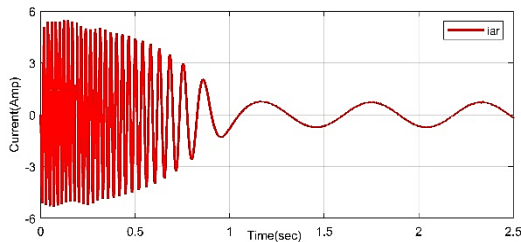


Figure 21. IM rotor current

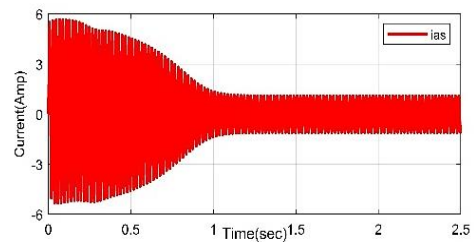


Figure 22. IM stator current

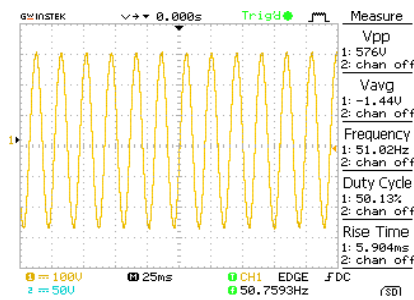


Figure 23. V_{pp} at 50 Hz

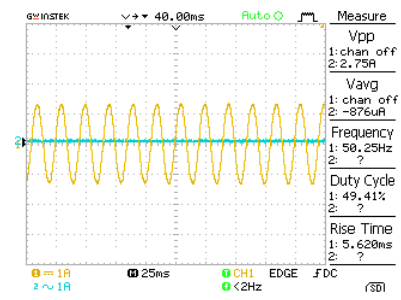


Figure 24. Line current at 50 Hz

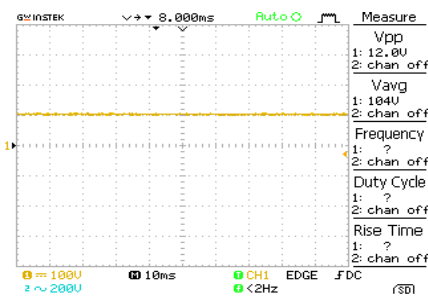


Figure 25. PV voltage at 1.5 pm

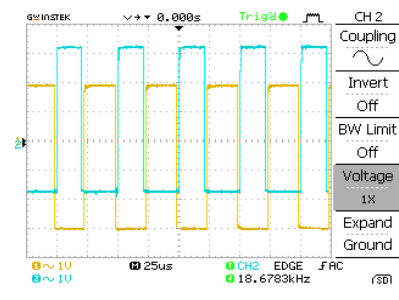


Figure 26. Part of S2 and S5 SPWM

4. CONCLUSIONS

An easy-to-use but effective PV standalone system is shown in this study. Utilizing MATLAB/Simulink, it models each component, simulates the entire system, and deals with radiation and temperature. The primary goal is to develop a cost-effective system that can be applied in a variety of industries by controlling the speed of the induction motor utilizing solar energy and fewer components. An economic analysis of an independent PV system was conducted, and the value of PV systems modules (PV, filter, and inverter). With the aid of PWM pulses generated by the SPWM system, this system uses an SSI inverter to convert DC voltage acquired from PV to AC voltage gained by driving specially designed IGBTs switches. The INC technique is utilized to complete the MPPT computation in order to extract the most power possible from the PV array. Use the V/f control to more effectively start and regulate the speed of instant messaging. The computer's MATLAB/Simulink interfaces are constructed using real hardware. The system's simulation results are well-aligned with the corresponding experimental setups. This work has led to the conclusion that this system can be employed in a variety of ways to generate clean, environmentally friendly energy.

REFERENCES



- [1] C. Sachin and K. B. Shah, "Solar photovoltaic fed induction motor for water pumping system using MPPT algorithm," *International Journal of Electrical and Electronics Engineering (IJEET)*, vol. 7, no. 3, pp. 31–42, Apr. 2018.
- [2] V. S Prasad Rao K, N. C. Kodavatiganti, and A. V. Ravikumar, "PV based agricultural pumping system using boost inverter fed induction motor," *International Journal of Recent Technology and Engineering (IJRTE)*, vol. 8, no. 3, pp. 8937–8941, Sep. 2019, doi: 10.35940/ijrte.C5386.098319.
- [3] M. A. Senol, "Solar powered hybrid multilevel inverter fed induction motor using fuzzy proportional integral speed controller," *Thermal Science*, vol. 23, no. 1, pp. 391–402, Jan. 2019, doi: 10.2298/TSCI180909052S.
- [4] G. Ramesh, K. Vasavi, and S. L. Sirisha, "Photovoltaic cell fed 3-phase induction motor using mppt technique," *International Journal of Power Electronics and Drive Systems (IJPEDS)*, vol. 5, no. 2, pp. 203–210, Oct. 2019, doi: 10.11591/ijpeds.v5i2.6209.
- [5] S. H. Darweesh, and W. I. Al-Rijabo, "Study of spatial variation of total solar radiation falling on horizontal surface in Iraq," *Al-Rafidain Science Journal*, vol. 22, no. 4, pp. 119–134, 2011, doi: 10.33899/rjs.2011.6794.
- [6] D. Verma, S. Nema, A. M. Shandilya, and S. K. Dash, "Maximum power point tracking (MPPT) techniques: Recapitulation in solar photovoltaic systems," *Renewable and Sustainable Energy Reviews*, vol. 54, pp. 1018–1034, 2016, doi: 10.1016/j.rser.2015.10.068.
- [7] D. K. Sharma, and G Purohit, "Advanced perturbation and observation (P&O) based maximum power point tracking (MPPT) of a solar photo-voltaic system," in *5th IEEE Int. Conf., on Power Electronics*, India, 2012, doi: 10.1109/IICPE.2012.6450411.
- [8] A. H. Mutlag, A. Mohamed, and H. Shareef, "An improved perturbation and observation based maximum power point tracking method for photovoltaic systems," *Jurnal Teknologi*, vol. 78, no. 6, pp. 19–25, 2016, doi: 10.11113/jt.v78.8887.
- [9] A. Al Tarabsheh, M. Akmal, and M. Ghazal, "Series connected photovoltaic cells-modelling and analysis," *Sustainability*, vol. 9, no. 3, p. 371, 2017, doi: 10.3390/su9030371.
- [10] T. F. Chan, and K. Shi, "Applied intelligent control of induction motor drives," 1st, vol.1, John Wiley & Sons, vol. 1, IEEE PRESS 2011, pp. 1-3.
- [11] K. S. Nithin, B. M. Jos, and M. Rafeek, "An improved method for starting of induction motor with reduced transient torque pulsations," *Int. Journal of Advanced Research in Electrical, Electronics and Instrumentation Eng.*, vol. 2, no. 1, pp. 462–470, 2013.
- [12] Y. Siwakoti, F. Z. Peng, F. Blaabjerg, P. C. Loh, and G. Town, "Impedance-source networks for electric power conversion part i: A topological review," *IEEE Transactions on Power Electronicson*, vol. 30, no. 2, pp. 699–716, 2015, doi: 10.1109/TPEL.2014.2313746.
- [13] F. Al Juheshi, "Design and simulation a novel three-phase, five level inverter topology," M.S. thesis, Architectural Eng., Nebraska Univ., Lincoln, 2017.
- [14] S. Hegde, S. Angadi, and A. B. Raju, "Speed control of 3-phase induction motor using volt/hertz control for automotive application," in *Int. Conf., on Circuits, Controls, Communications and Computing (I4C)*, Bangalore, India, 2016, doi: 10.1109/CIMCA.2016.8053311.
- [15] G. L. Calzo, A. Lidozzi, L. Solero, and F. Crescimbin, "LC filter design for on-grid and off-grid distributed generating units," *IEEE Transactions on Industry Applications*, vol. 51, no. 2, pp. 1639–1650, 2015, doi: 10.1109/TIA.2014.2345952.
- [16] A. Moubarak, G. El-Saady, and E.A. Ibrahim, "Power quality improvement of photovoltaic water pumping system using LC filter," *ARNP Journal of Eng. and Applied Sciences*, vol. 13, no. 4, pp. 1311–1326, 2018.
- [17] M. G. Wanzeller, R. N. C. Alves, J. V. da Fonseca Neto, and W. A. dos Santos Fonseca, "Current control loop for tracking of maximum power point supplied for photovoltaic array," *IEEE Transactions on Instrumentation and Measurement*, vol. 53, no. 4, pp. 1304–1310, 2004, doi: 10.1109/TIM.2004.831166.
- [18] K. S. Gaeid, H. W. Ping, and H. A. F. Mohamed, "Indirect vector control of a variable frequency induction motor drive (VCIMD)," *ICICI-BME Proceedings*, 2009, pp. 36–40, doi: 10.1109/ICICI-BME.2009.5417273.
- [19] H. Z. Ali., A. AL-Salihi, and A. K. AL-Abodee, "Mapping monthly average global solar radiation over Iraq using GIS and heliosat model," *International Journal of Computers & Technology*, vol. 15, no. 5, pp. 6724–6731, 2016, doi: 10.24297/ijct.v15i5.1635.
- [20] V. Korde, N. Sute, V. B. Borghate, and V. M. Korde, "Analysis of control techniques and filter design of multilevel inverter," in *Smart Technologies for Energy, Environment and Sustainable Development*, vol. 2, pp 571–588, 2022.
- [21] A. Bhanuchandar, and B.K Murthy, "A new single-phase five-level self-balanced and boosting grid-connected switched capacitor inverter with LCL filter," in *Sustainable Energy and Technological Advancements*, Advances in Sustainability Science and Technology. Springer, Singapore.
- [22] G.M.Cocco, F.B. Grigolett, L.G. Scherer, et al., "Modeling and control of hydro-pv hybrid power system with three-phase three-leg split-source inverter," *Journal Control Autom Electr Syst.*, vol. 33, pp. 1563–1575, 2022, doi: 10.1007/s40313-022-00911-4.
- [23] [https://www.fullversiondl.com/proteus-professional-v8-9-sp2-build-28501-library/Labcenter.Electronic limited.accessed date](https://www.fullversiondl.com/proteus-professional-v8-9-sp2-build-28501-library/Labcenter.Electronic%20limited.accessed%20date).

January 11, 2020.



- [24] "Mainstream Mixed signals MCUs Arm Cortex-M4 core with DSP and FPU, 64 Kbytes of Flash memory, 72 MHz CPU, CCM, 12-bit ADC 5 MSPS, comparators, op-amp, hr timer," 2018. [Online]. Available: <https://www.st.com/en/microcontrollers-microprocessors/stm32f334r8.html>, 2022.
- [25] D. Urukalo, and Ž. V. Despotović, "Experimental verification of electrical power consumption of resonant electromagnetic vibratory feeder," *19th International Symposium INFOTEH-JAHORINA (INFOTEH)*, 2020, pp. 1-5, doi: 10.1109/INFOTEH48170.2020.9066331.

BIOGRAPHIES OF AUTHORS






Omer N. Mahmmoud   received his Master's degree in Electrical Engineering from Tikrit University, Iraq, in 2021. He also obtained a Bachelor of Engineering (Electrical Engineering) from Tikrit University, Iraq in 2006. He is currently an Assistant Lecturer in the Department of Electrical Engineering, Tikrit University, Iraq. Since 2006 he has been working as an engineer in the laboratories of the Electrical Engineering Department at Tikrit University. He can be contacted at email: eng.omernafaa2016@gmail.com.





Salam R. Mahdi   received B.Sc. degree in Mathematics Science from College of Science/Baghdad University, Baghdad-Iraq, in 1990, and the Higher Diploma degree in Computer science from Iraqi Commission for Computers and Informatics/ Informatics Institute for Post Graduate Studies, Baghdad Iraq in 1999, and received Master degree in Computer science from Iraqi Commission for Computers and Informatics / Informatics Institute for Post Graduate Studies, Baghdad Iraq in 2005. He Graduated PhD Doctoral degree in Informatics Engineering/Computer Engineering from Aleppo University Aleppo-Syria, Electrical & Electronic Engineering College, Department of Computer Engineering in 2015. His Doctoral research was in the Development new methods keystreams generating in stream cipher for information hiding. He is Senior Lecturer, and Owner and Manager of RAM General Express LLC, and Home Health Care LLC in Ohio USA. He is IEEE Senior member in USA. He can be contacted at email: mr_salam4@yahoo.com.



Khalaf S. Gaeid    received the B.Sc. degree in electrical engineering/Control from MEC, Baghdad, Iraq in 1993 and the M.Sc. degree in Control Engineering from University of Technology, Baghdad, Iraq in 2004. He graduated from University of Malaya, Malaysia in 2012 with the PhD degree in control system and machine drives. His doctoral research was in the development new fault tolerant controller-based wavelet for induction machines. He is currently professor in control systems at the Department of Electrical Engineering, College of Engineering, Tikrit University, Tikrit, Iraq. His research interests include fault tolerant control, wavelet, fault diagnosis, machine drives and their applications in electrical engineering. He is IEEE member with many publications in high rank journals and conferences. He can be contacted at email: gaeidkhalaf@gmail.com.



Atheer L. Salih Al-Tameemi   holds a Bachelor of Engineering (B.Eng.) in Electronics and Communications Engineering from University of Baghdad-Iraq, a Master of Engineering Science (M.Eng.Sc.) in Control System Engineering from the University of Malaya in Kuala Lumpur-Malaysia, and holds a (Ph. D.) degree in Electrical Engineering in Image and Signal Processing from the Technical University of Dortmund-Germany. He is currently a research staff member and lecturing in the field of Electrical Engineering at Baden-Wuerttemberg Cooperative State University at the campus of Friedrichshafen-Germany. He works in different areas of research within Electrical Engineering. Research Interests: Simulation, Image Processing, Communication Engineering, Wave Propagation, Control systems, EMC Systems and Artificial Intelligence. Address: Baden-Wuerttemberg Cooperative State University (DHBW) Ravensburg, Campus Friedrichshafen, Fallenbrunnen 2, 88045 Friedrichshafen, Germany. Tel. +49-7541-2077-227. He can be contacted at email: al-tameemi@dhbw-ravensburg.de.